



ISSN 1001-0742
CN 11-2629/X

2012

Volume **24**
Number **4**

JOURNAL OF
**ENVIRONMENTAL
SCIENCES**



Sponsored by
Research Center for Eco-Environmental Sciences
Chinese Academy of Sciences

CONTENTS

Aquatic environment

- Comparison of conventional and inverted A²/O processes: Phosphorus release and uptake behaviors
Rong Qi, Tao Yu, Zheng Li, Dong Li, Takashi Mino, Tadashi Shoji, Kochi Fujie, Min Yang 571
- Distribution of heavy metals in sediments of the Pearl River Estuary, Southern China: Implications for sources and historical changes
Feng Ye, Xiaoping Huang, Dawen Zhang, Lei Tian, Yanyi Zeng 579
- Removal of arsenate and arsenite from aqueous solution by waste cast iron
Nag-Choul Choi, Song-Bae Kim, Soon-Oh Kim, Jae-Won Lee, Jun-Boum Park 589
- Effect of artificial aeration on the performance of vertical-flow constructed wetland treating heavily polluted river water
Huiyu Dong, Zhimin Qiang, Tinggang Li, Hui Jin, Weidong Chen 596
- A 60-year sedimentary record of natural and anthropogenic impacts on Lake Chenghai, China
Fengyu Zan, Shouliang Huo, Beidou Xi, Jingtian Zhang, Haiqing Liao, Yue Wang, Kevin M. Yeager 602
- Preparation and application of amino functionalized mesoporous nanofiber membrane via electrospinning for adsorption of Cr³⁺ from aqueous solution
Ahmed A. Taha, Junlian Qiao, Fengting Li, Bingru Zhang 610
- Removal of phosphate ions from aqueous solution using Tunisian clays minerals and synthetic zeolite
Noureddine Hamdi, Ezzeddine Srasra 617

Atmospheric environment

- Impacts of continuously regenerating trap and particle oxidation catalyst on the NO₂ and particulate matter emissions emitted from diesel engine
Zhihua Liu, Yunshan Ge, Jianwei Tan, Chao He, Asad Naeem Shah, Yan Ding, Linxiao Yu, Wei Zhao 624
- Dry deposition velocity of total suspended particles and meteorological influence in four locations in Guangzhou, China
Leifu Chen, Shaolin Peng, Jingang Liu, Qianqian Hou 632
- Synthesis, characterization and experimental investigation of Cu-BTC as CO₂ adsorbent from flue gas
Jiangkun Xie, Naiqiang Yan, Zan Qu, Shijian Yang 640
- Aerosol effects on ozone concentrations in Beijing: A model sensitivity study
Jun Xu, Yuanhang Zhang, Shaoqing Zheng, Youjiang He 645
- Measurement of air exchange rates in different indoor environments using continuous CO₂ sensors
Yan You, Can Niu, Jian Zhou, Yating Liu, Zhipeng Bai, Jiefeng Zhang, Fei He, Nan Zhang 657
- Influence of different weather events on concentrations of particulate matter with different sizes in Lanzhou, China
Xinyuan Feng, Shigong Wang 665

Terrestrial environment

- Sorption of chlorophenols onto fruit cuticles and potato periderm
Yungui Li, Yingqing Deng, Baoliang Chen 675
- Effects of urea and (NH₄)₂SO₄ on nitrification and acidification of Ultisols from Southern China
Deli Tong, Renkou Xu 682
- Health risk assessment of heavy metals in soils and vegetables from wastewater irrigated area, Beijing-Tianjin city cluster, China
Yanchun Wang, Min Qiao, Yunxia Liu, Yongguan Zhu 690
- PCDD/Fs in soil around a hospital waste incinerator: comparison after three years of operation
Xiaodong Li, Mi Yan, Jie Yang, Tong Chen, Shengyong Lu, Jianhua Yan 699
- Dissolved organic sulfur in streams draining forested catchments in southern China
Zhanyi Wang, Xiaoshan Zhang, Zhangwei Wang, Yi Zhang, Bingwen Li, Rolf Vogt 704

Environmental biology

- Ammonium-dependent regulation of aerobic methane-consuming bacteria in landfill cover soil by leachate irrigation
Fan Lü, Pinjing He, Min Guo, Na Yang, Liming Shao 711
- Steady performance of a zero valent iron packed anaerobic reactor for azo dye wastewater treatment under variable influent quality
Yaobin Zhang, Yiwen Liu, Yanwen Jing, Zhiqiang Zhao, Xie Qian 720
- Identification of naphthalene metabolism by white rot fungus *Armillaria* sp. F022
Tony Hadibarata, Abdull Rahim Mohd Yusoff, Azmi Aris, Risky Ayu Kristanti 728

Environmental health and toxicology

- Inhibition of ROS elevation and damage to mitochondrial function prevents lead-induced neurotoxic effects on structures and functions of AFD neurons in *Caenorhabditis elegans*
Qiuli Wu, Peidang Liu, Yinxia Li, Min Du, Xiaojuan Xing, Dayong Wang 733

Environmental catalysis and materials

- Photodegradation of Norfloxacin in aqueous solution containing algae
Junwei Zhang, Dafang Fu, Jilong Wu 743
- Synthesis of TiO₂ nanoparticles in different thermal conditions and modeling its photocatalytic activity with artificial neural network
Fatemeh Ghanbary, Nasser Modirshahla, Morteza Khosravi, Mohammad Ali Behnajady 750
- Preparation of Fe_xCe_{1-x}O_y solid solution and its application in Pd-only three-way catalysts
Jianqiang Wang, Meiqing Shen, Jun Wang, Mingshan Cui, Jidong Gao, Jie Ma, Shuangxi Liu 757
- Dechlorination of chlorophenols by zero valent iron impregnated silica
Praveena Juliya Dorathi, Palanivelu Kandasamy 765
- Photocatalytic degradation of perfluorooctanoic acid with β-Ga₂O₃ in anoxic aqueous solution
Baoxiu Zhao, Mou Lv, Li Zhou 774

Serial parameter: CN 11-2629/X*1989*m*210*en*P*27*2012-4



Removal of phosphate ions from aqueous solution using Tunisian clays minerals and synthetic zeolite

Noureddine Hamdi*, Ezzeddine Srasra

National Center of Research in Materials Sciences, Borj Cedria Technopole 95-2050, Tunisia. E-mail: hamdinoureddine@yahoo.fr

Received 08 February 2011; revised 12 May 2011; accepted 21 June 2011

Abstract

Phosphate ions are usually considered to be responsible for the algal bloom in receiving water bodies and aesthetic problems in water. From the environmental point of view, the management of such contaminant and valuable resource is very important. The present work deals with the removal of phosphate ions from aqueous solutions using kaolinitic and smectic clay minerals and synthetic zeolite as adsorbent. The pH effect and adsorption kinetic were studied. It was found that phosphate could be efficiently removed at acidic pH (between 4 and 6) and the second order model of kinetics is more adopted for all samples. The isotherms of adsorption of phosphate ions by the two clays and the zeolite samples show that the zeolite has the highest rate of uptake (52.9 mg P/g). Equilibrium data were well fitted with Langmuir and Freundlich isotherm.

Key words: phosphate; adsorption; clay mineral; zeolite

DOI: 10.1016/S1001-0742(11)60791-2

Introduction

Phosphate discharged into the surface waters stimulates the growth of aquatic micro and macro organisms in nuisance quantities, which in excess can cause eutrophication in stagnant water bodies. Therefore, wastes containing phosphates must meet the discharge limits for phosphates, which are 0.5–1.0 mg/L according to the World Health Organization (WHO, 1993). In order to meet effluent quality standards, further treatment of secondary effluent is required. In wastewater treatment technology, various techniques have been used for phosphate removal. Coagulation-precipitation and biological process are widely accepted methods of phosphate removal at industrial level. Besides, the application of low cost and easily available materials in wastewater treatment has been widely investigated during recent years, such as fly ash (Agyei et al., 2002), blast furnace slag (Johansson and Gustafsson, 2000; Oguz, 2004), red mud (Akay et al., 1998), aluminium hydroxide (Guan et al., 2007), clays (Ye et al., 2006) and zeolites (Onyango et al., 2007). In general, these adsorbents were used for remove phosphate ions from wastewater at low concentration. The adsorption study of phosphate at higher concentration (≈ 1000 mg/L) has not been reported before. In this condition, the efficiency of some materials as sorbent of phosphate ions is required to use them as landfill liner in waste discharge site (Mitchell et al., 2000). In this situation clay mineral is one of the essential materials used to reduce

hydraulic conductivity and pollutant migration (Peterson and Gee, 1985). In addition, the synthesized zeolites were considered as a good adsorbent and can be used as thin film liner with clays minerals (Wu et al., 2006). Peolite is a promising alternative because of its low cost, selectivity and compatibility with the natural environment. Zeolite is framework aluminosilicate with pore dimensions of molecular sizes generated by corner-sharing Al^{3+} and Si^{4+} oxygen tetrahedra. Due to synthetic zeolite having uniform micropore structure and high surface area, it usually has a higher adsorption capability compared with clay minerals. Therefore, to obtain low-cost and effective synthetic zeolite, many researchers have investigated the synthesis of zeolite from fly ash, metakaolinite, and chrysotile etc. (Wu et al., 2006; Saada et al., 2009; Juan et al., 2009; Youssef et al., 2008; Petkowicz et al., 2008). However, in many of these studies, the total conversion time was generally long (24–72 hr or more); the synthesis temperature was high (90–180°C); and the synthetic zeolite products still contained a significant amount of residual raw materials and/or other phases. The presence of nonzeolitic phases in the converted products limits the cation exchange capacity of the products and greatly reduces the applicability of synthetic zeolite. Therefore, developing effective, high adsorption capacity and low-cost synthetic zeolite for phosphate removal continues to be a great challenge.

In this study, three sorbents (two clays and synthetic zeolite prepared from kaolinite) were then characterized and their phosphate adsorption behaviour was studied under varying experimental conditions such as pH, time

* Corresponding author.

effect and initial concentration. The results are presented in terms of sorption kinetics and equilibrium isotherm that are fitted by Langmuir and Freundlich models.

1 Experimental

1.1 Raw materials

The clays samples (T and G) used in this study were provided from Tabarka (North West of Tunisia) and Gabes (South East of Tunisia), respectively.

The X-ray diffraction analysis of both samples (Fig. 1) indicated that the mineralogical composition of clay T is mainly composed of kaolinite and illite the impurity is the quartz. In the case of clay H (Fig. 1) the main fractions are smectite and kaolinite associated to quartz and calcite. To illuminate these impurities from clay fraction, the raw powder sample were saturated with Na⁺ by five washing cycles (successive centrifugal treatments) with 1 mol/L NaCl solution. After each centrifugation of the suspension, the supernatant was discarded and replaced with a fresh solution of NaCl. After that, the recuperated samples were dialysed through a specific membrane until free from Cl⁻, dried at 80°C and finally the purified clays will be used for

phosphate adsorption.

1.2 Preparation of zeolite

A conventional alkaline fusion method was used for the synthesis of zeolite from purified clay T. Approximately 10 g clay powder were mixed with 12 g NaOH, then were placed in the furnace with 600°C for 1 hr. The powder recuperated after calcinations were dissolved in 85 mL of distilled water agitated during 24 hr. The mixture crystallized in teflon bottle at three temperatures (70, 90 and 110°C) for 12 hr. Solid powder was filtered-off, washed, dried at 80°C for 12 hr and the product was obtained.

1.3 Characterization

The clay samples and prepared zeolites were characterized by XRD, cationic exchange capacity (CEC), specific surface area (S_{BET}) and SEM. Powder XRD patterns were obtained using a PANalytical X'Pert HighScore Plus diffractometer (the Netherlands) in the 2 θ range 3–40°, at a scanning rate of 2°/min and employing CuK α filtered radiation. The cationic exchange capacity (CEC) of sample was determined using ammonium acetate method (Van Reeuwijk, 1992). The specific surface area S_{BET} was measured at 77 K by the BET method with a Quantachrome Autosorb-1 instrument (USA) using N₂ gas. The morphological observation of zeolite powder was undertaken using a Philips Fei Quanta 200 scanning electron microscope (the Netherlands).

1.4 Phosphate adsorption experiments

The batch experiments were carried out in polyethylene bottles containing 30 mL varying initial concentrations of phosphorus solutions and 0.2 g of adsorbent (clays or zeolite). Then the samples were agitated in a thermostatic orbital shaker with a shaking of 200 r/min at ambient temperature. On reaching equilibrium the adsorbent was eliminated by centrifugation at 3000 r/min. The suspension was adjusted to desired pH levels by adding NaOH (0.1 or 0.01 mol/L) or HCl (0.1 or 0.01 mol/L) solution.

The initial and final phosphate concentrations remaining in solutions were analyzed using the standard method (vanadomolybdophosphoric acid colorimetric method, 1998) using a Hach DR/4000 spectrophotometer (USA).

The amount of phosphate adsorbed at equilibrium (Q_{ad} , mg/g) was calculated by using the following:

$$Q_{ad} = \frac{(C_0 - C_{eq}) \times V_s}{m} \quad (1)$$

where, C_0 (mg/L) and C_{eq} (mg/L) are the initial and equilibrium concentrations of phosphate solution, respectively; V_s (L) is the volume of phosphate solution and m (g) is the weight of sorbent (clays or zeolite).

2 Results and discussion

2.1 Characterization of purified clays and synthetic zeolites

Figure 2a shows the diffractogram patterns of oriented pure clay T, we observe in the presence of illite at 10 Å and the

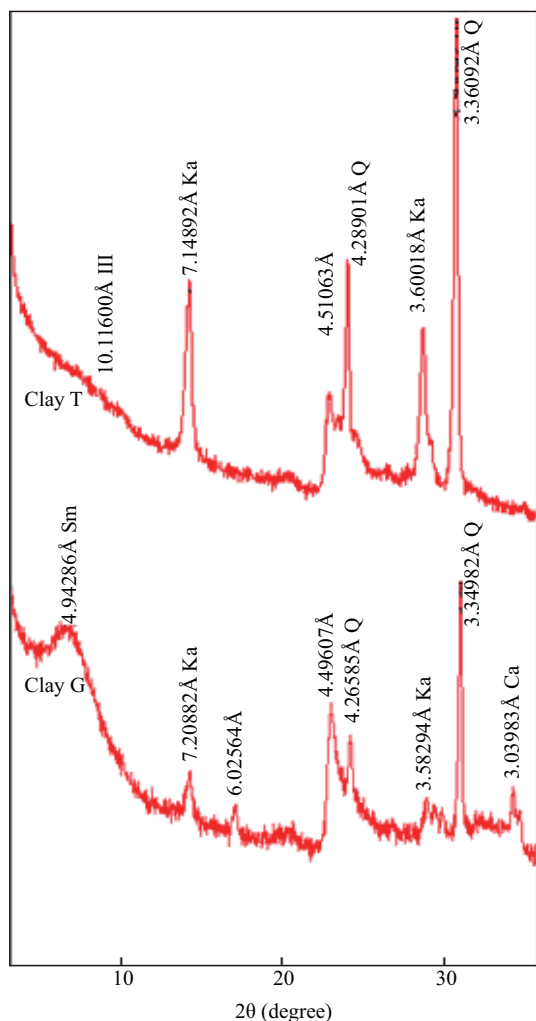


Fig. 1 X-ray diffraction patterns of powder samples of clay T, and clay G. Ill: illite, Ka: kaolinite, Sm: smectite, Q: quartz, Ca: calcite.

jesec.cn

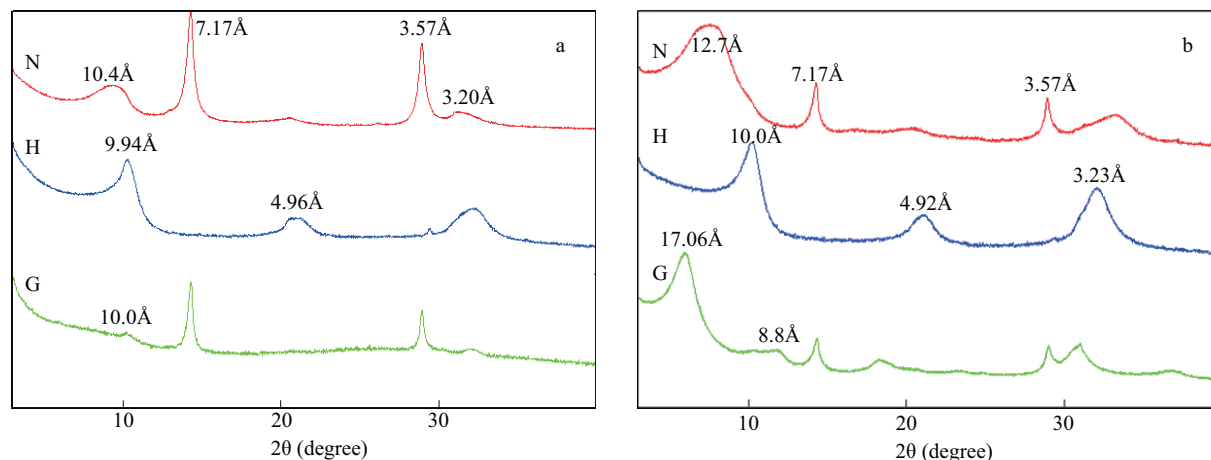


Fig. 2 X-ray diffraction patterns of the oriented clay T (a) and clay G (b) fractions (< 2 μm) (N: normal untreated, H: heated, and G: glycolated).

kaolinite at 7.17 Å which disappear after heating at 550°C.

The X-ray diffraction analysis of pure clay H (Fig. 2b) indicates the presence of smectite at 12.7 Å, after treatment by ethylene glycol the peak passed to 17.06 Å but the d_{002} appeared at 8.8 Å is attributable to an interstratified smectite-illite, also the presence of small amount of the kaolinite at 7.17 Å, which disappear after heating at 550°C.

Figure 3 shows the XRD patterns of the products synthesized at three temperatures (70, 90 and 110°C). The typical diffraction peaks corresponding to kaolinite and illite remarkably disappear. The diffractogramme of sample prepared at 70°C shows that all XRD peaks agree well with the characteristic peaks of zeolite 4A, syn ($\text{Na}_{11.5}\text{Al}_{11.5}\text{Si}_{12.5}\text{O}_{48}$) by comparing the d -values of the products obtained with JCPDS data of card No. 076-1042. No additional peaks are observed, indicating the crystallization of pure-form zeolite 4A. The XRD of the crystals has a low background, strong intensities and sharp peaks, indicating the as-synthesized zeolite 4A crystals are perfect.

This result is confirmed by the cubic crystalline structure with that well defined edge of the zeolite A particles can be readily observed in SEM image (Fig. 4). The particle size and average width of the product can be estimated, 1–1.2 μm and 1 μm, respectively. At the temperature of 90°C the synthesized product is mainly the zeolite 4A but at 110°C it is transformed to the sodalite zeolite (HS).

The S_{BET} and CEC value of clay samples and synthesized zeolites are shown in Table 1. After purification the CEC and S_{BET} of both clays increase, the sample G had the higher value, this is due to the smectic fraction. Besides, it is not surprising that the S_{BET} and the CEC values of zeolitized products increased drastically compared with the corresponding clay due to the formation of zeolite. The zeolite synthesized at 70°C shows the higher S_{BET} and CEC value comparing to others products. Therefore, the synthesized zeolite may be a promising material for the removal of phosphate from wastewater. The experiment of the removal of phosphate is now on the process of our investigation.

2.2 Phosphate immobilization by two clays and synthesized zeolite A (70°C)

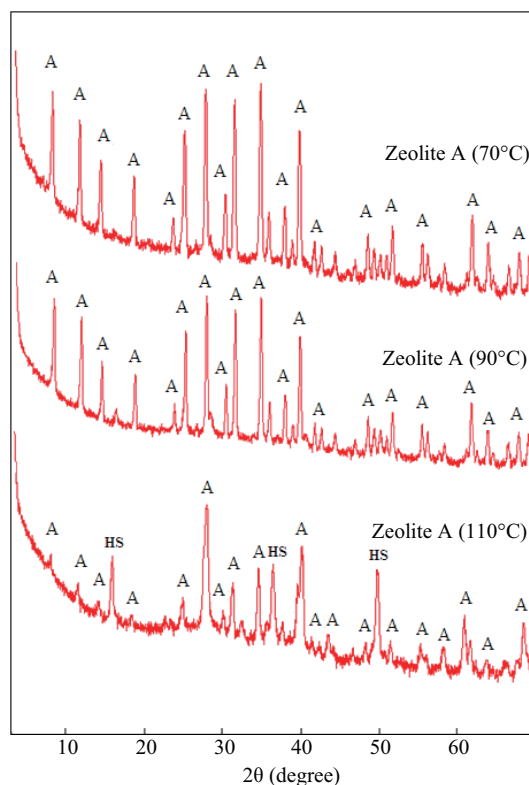


Fig. 3 XRD patterns of synthesized zeolites obtained from clay T at three temperatures (70, 90 and 110°C).

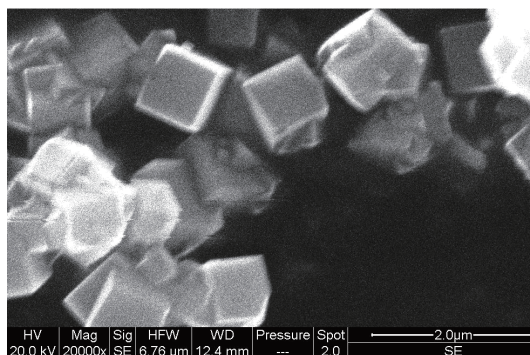


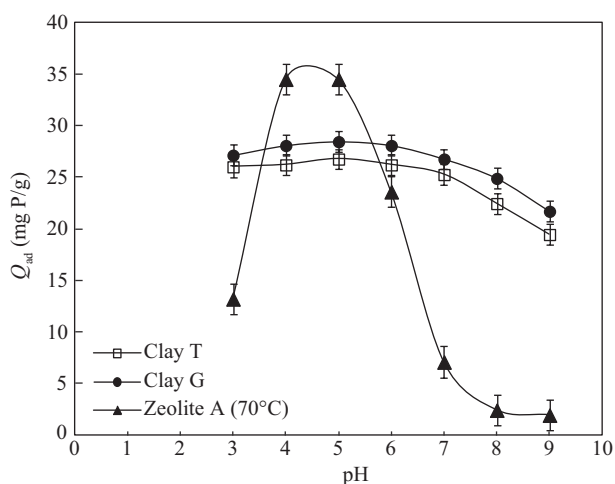
Fig. 4 SEM image of synthesized zeolite A obtained at 70°C.

2.2.1 Effect of pH

The pH of the aqueous solution is an important variable which controls the adsorption of the phosphate anions at

Table 1 Specific surface area and cationic exchange capacity of clay and zeolite samples

Sample	S_{BET} (m^2/g)		CEC (meq/100 g)	
	Raw	Purified	Raw	Purified
Clay T	35.3	68.5	16	24
Clay G	69.8	106.2	56	83
Zeolite 70°C		174.4		330
Zeolite 90°C		105.2		282
Zeolite 110°C		74.5		208

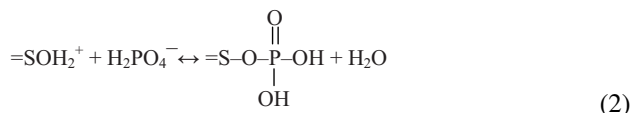
**Fig. 5** Effect of pH values for phosphate adsorption on two clays and synthesized zeolite A (70°C).

the clay or zeolite-water interfaces (Farrah and Pickering, 1977). Hence, the influence of pH on the adsorption of phosphate ions onto clay and zeolite samples was investigated in the pH range of 3.0–9.0. Figure 5 shows the effect of pH on adsorption of phosphate onto the two clays and the zeolite (70°C). It can be observed that the adsorption of phosphate ions by clay T and G increases weakly with an increase in pH to a maximum around pH 5, and then decreases as the pH becomes more basic due to the competition with OH^- . Clays are known to possess a negative surface charge in solution. As pH changes, surface charge also changes, and the adsorption of charged species is affected. The same result was found for montmorillonite clay by Zhu et al. (2009). Besides, the adsorptions of anions like phosphate are favorable at pH lower than point of zero charge (PZC) of materials which is about (PZC = 5.7) for kaolinite and (PZC = 6.4) for smectite sample.

In the case of zeolite sample the maximum of adsorption was found between pH 4 and pH 5, the same curve form was observed by Chen et al. (2006). However, in this range of pH the zeolite shows a higher uptake ability of phosphate comparing to others samples, which may be due to a greater number of surface sites with a PZC = 5.5, also the zeolite A has a three-dimensional structure and higher surface area.

The adsorption mechanisms of phosphate anions by clay and zeolite at acidic pH are relatively complex. Reed et al. (2000) identified two forces that play a role in an adsorption process, the first is chemical interaction and the second is the electrostatic forces. The latter gives rise to Coulombic attraction or repulsion between binding

sites and adsorbing ions. To understand how these forces affected the phosphate sorption behavior, the following reaction is considered (Eq. (2)), with S represents the element at the surface of clay or zeolite, and generally is the Aluminum (Al).



In the case of phosphate anions at acidic condition (pH from 3 to 5), the dominate fraction in solution is the negative monovalent H_2PO_4^- (Hartley et al., 1997). Besides, some binding sites are protonated (SOH_2^+) at such pH values. Consequently, a higher Coulombic attraction between the binding sites and H_2PO_4^- ions (Eq. (2)) in addition to chemical interaction (or molecular adsorption) leads to a higher phosphate uptake.

2.2.2 Phosphate adsorption kinetics

The results of phosphate adsorption kinetic experiments at room temperature and for a concentration of 500 mg P/L are shown in Fig. 6. It can be seen that the majority of phosphate adsorption on the adsorbents were completed in 2 hours. However, the two clays have faster kinetics than the synthetic zeolite, which can be attributed to the delay of adsorption in the zeolitic cavity.

In this study, the P adsorption kinetic data were fitted with the two kinetic models (the first- and second-order kinetic).

The linear form of the pseudo first-order equation is given by Eq. (3):

$$\log(Q_e - Q_t) = \log Q_e - K_1 t \quad (3)$$

The linear form of the pseudo second-order model (Nghah and Fatinathan, 2010) is given by Eq. (4):

$$\frac{t}{Q_t} = \frac{1}{k_2 Q_e^2} + \frac{1}{Q_e} t \quad (4)$$

where, Q_e (mg/g) and Q_t (mg/g) refer to the amount of phosphate ions adsorbed at equilibrium and at any time, t (min), respectively, and k_1 (hr^{-1}) is the equilibrium rate

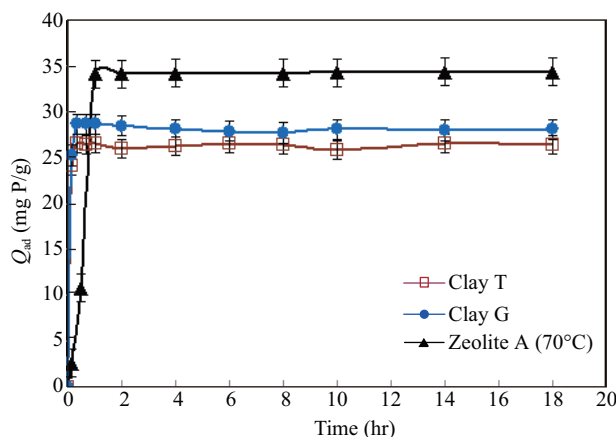
**Fig. 6** Effect of contact time for phosphate adsorption on clays and synthesized zeolite A (70°C).

Table 2 Comparison of the pseudo first- and second-order adsorption rate constants, at constant concentration of phosphate 500 mg P/L

Sample	First-order kinetic model			Second-order kinetic model		
	k_1 (hr ⁻¹)	Q_e (mg P/g)	R^2	k_2 (g/(mg·hr))	Q_e (mg P/g)	R^2
Clay T	0.027	0.23	0.0134	2.87	26.38	0.9998
Clay G	0.07	0.24	0.1273	21.2	28.01	0.9999
Zeolite 70°C	0.086	1.60	0.4135	0.19	36.36	0.9908

constant of pseudo first-order kinetics and k_2 (g/(mg·hr)) is the equilibrium rate constant of pseudo second-order kinetics.

Therefore, the resulting from both models equations show the high applicability of the second-order equation for the present kinetic data for all samples (Fig. 7). The correlation coefficients calculated for all models, i.e., R^2 , and the other parameters are shown in Table 2. It was observed that correlation coefficient, R^2 , for the pseudo first-order model was much lower (< 0.90) than for the pseudo second-order kinetic models. While the calculated equilibrium sorption capacity ($Q_{e,calc}$) for the first-order model is not close to the experimental values ($Q_{e,exp}$), whereas for the second-order model, $Q_{e,calc}$ values are close to $Q_{e,exp}$ for the initial concentration.

2.2.3 Phosphate adsorption isotherms

Equilibrium studies were carried out to determine the optimum conditions for maximum phosphate ions removal by these three samples. The experimental sorption isotherm is used to plot the amount of P sorbed, expressed in mg P/g sample against the equilibrium phosphate ions concentration (mg/L). The experimental sorption data for the removal of phosphate ions were correlated with Langmuir (Eq. (5)) and Freundlich (Eq. (6)) models.

$$Q_e = \frac{Q_m b C_e}{1 + b C_e} \quad (5)$$

$$Q_e = K_F C_e^{1/n} \quad (6)$$

where, Q_e (mg/g) is the amount of ions adsorbed per unit weight of adsorbents, C_e (mg/L) is the equilibrium concentration, Q_m and b are the Langmuir constants related

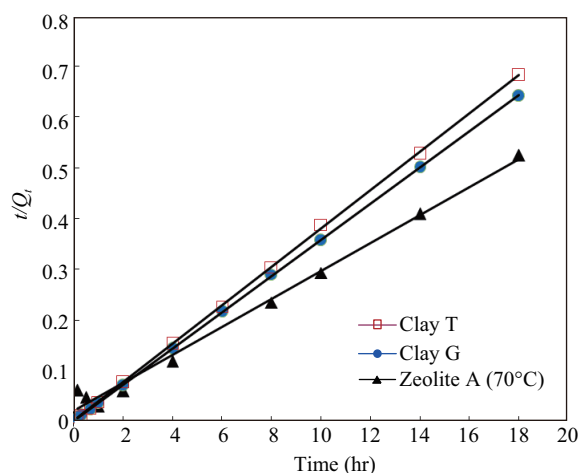


Fig. 7 Pseudo second-order kinetic plots for the adsorption of phosphate ions onto clays and zeolite samples.

to capacity and energy of adsorption, respectively. K_F and $1/n$ are the Freundlich constants.

Based on the results of the kinetic and pH studies, all equilibrium experiments were carried out at pH (5.0 ± 0.2) and for a reaction period of 4 hr using the KH_2PO_4 solution at various concentrations (50 to 1000 mg P/L). The isotherms of phosphate adsorption onto clays and zeolite at room temperature are shown in Fig. 8. In the low concentration region, the amount of phosphate adsorbed on the samples sharply increased with an increase in equilibrium concentration, giving an indication of the high affinity of the binding sites for phosphate ions. This is a good attribute of the materials tested in this study since a high uptake at low equilibrium concentration will enable the treatment of a large volume of water before replacement or regeneration of the adsorbents. At high concentration, the increase in quantities adsorbed is gradual as a result of an almost full occupancy of the active sites. Figure 8 shows that the zeolite has the higher adsorption capacity of phosphate ions.

The experimental sorption data of the adsorption of phosphorous were correlated with Langmuir and Freundlich models. Figure 9 shows that the linear Langmuir and Freundlich equations give a good fit to the adsorption isotherm for the sorption of phosphate ions onto clays and zeolite. It is shown that the experimental data of phosphate adsorption on these samples could be well matched by the Freundlich isotherms and the zeolite had high adsorption quantity 52.9 mg P/g (Table 3).

2.2.4 Comparison of phosphate removal with different adsorbents reported in literature

The adsorption capacities of these adsorbents (two clays and zeolite A) for the removal of phosphate have been compared with those of other adsorbents reported in lit-

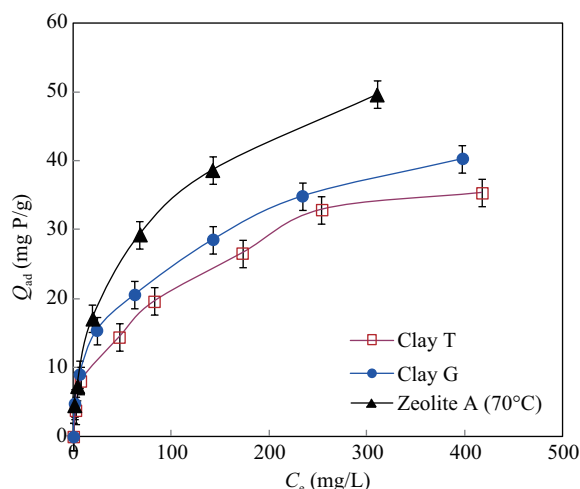
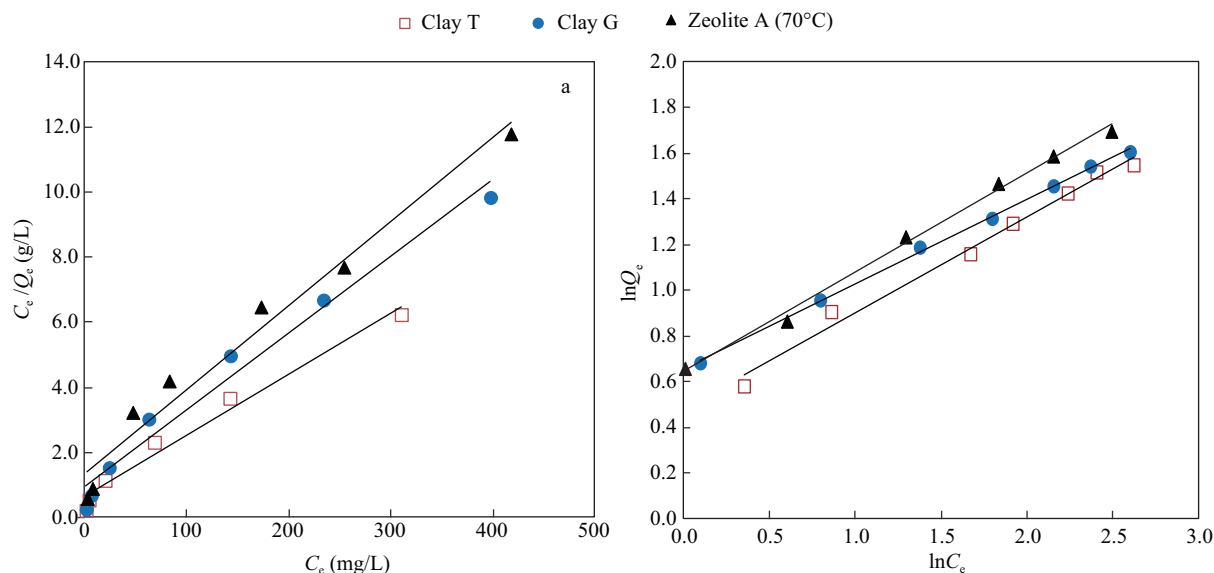


Fig. 8 Phosphate adsorption isotherms.

Table 3 Estimated isotherms parameters for phosphate adsorption

Sample	Langmuir model			Freundlich model		
	Q_m (mg P/g)	b	R^2	K_F	$1/n$	R^2
Clay T	38.46	0.0184	0.9712	3.07	0.408	0.9878
Clay G	42.19	0.0259	0.9762	4.61	0.369	0.9959
Zeolite 70°C	52.91	0.0292	0.9779	4.40	0.434	0.9950

**Fig. 9** Linear plot of Langmuir isotherm (a) and Freundlich isotherm (b) for the adsorption of phosphate ions onto two clays and zeolite.**Table 4** Adsorption capacity of phosphate on some adsorbents

Adsorbent	Q_{max} (mg/g)	Reference
Modified palygorskite clay	8.31	Ye et al., 2006
Precipitator fly ash	13.76	Cheung and Venkitachalam, 2000
Blast furnace slag	44.24	Sakadevan and Bavor, 1998
Lithium intercalated gibbsite	93	Wang et al., 2007
Kaolinitic clay	38.46	This study
Smectic clay	42.19	This study
Zeolite A	52.91	This study

erature and the values of adsorption capacities have been presented in Table 4. The adsorption capacity varies and it depends on the characteristics of the individual adsorbent the value of PZC, the number of surface sites or the precipitation of phosphate compound at basic pH. For example, in the case of the lithium intercalated gibbsite and blast furnace slag the presence of calcium in substrates may improve the removal capacity of phosphate by both adsorption and precipitation (Wang et al., 2007; Sakadevan and Bavor, 1998).

Another concern is the cost when kaolinite and smectite clays and synthetic zeolite are used to remove phosphate. These clays minerals are collected from natural deposit abundant in Tunisia. Also the zeolite was synthesized from the clay T with a conventional alkaline fusion method. This method is very simple with low cost. In addition, compared with palygorskite, sepiolite and other mineral materials (Nandi et al., 2008), the price of kaolinite and smectite is lower than that of them. Anyway, these two clays and the

zeolite may be a relatively low cost treatment option for phosphate from aqueous solution.

3 Conclusions

In this study, pure form, single phase and highly crystalline zeolite A was successfully synthesized from Tunisian kaolinitic clay mineral at 70°C. This zeolite and two Tunisian clays minerals (smectite and kaolinite) were tested to remove phosphate ions from aqueous solution. The adsorption isotherms, kinetics, pH effect and thermodynamic parameters were examined.

The results show that all samples had faster kinetics and zeolite had the higher adsorption capacities, which can be attributed to the surface structural changes of the materials.

Both Langmuir and Freundlich models fit well with the experimental data and R^2 value of Freundlich model are higher than Langmuir model.

The relatively low cost and high capabilities of the two clays and zeolite make them potentially attractive adsorbents for the removal of phosphate from aqueous solution.

References

- Ageyi N M, Strydom C A, Potgieter J H, 2002. The removal of phosphate ions from aqueous solution by fly ash, slag, ordinary Portland cement and related blends. *Cement and Concrete Research*, 32(12): 1889–1897.
- Akay G, Keskinler B, Çakici A, Danis U, 1998. Phosphate removal from water by red mud using crossflow microfil-

- tration. *Water Research*, 32(3): 717–726.
- Chen J C, Kong H N, Wu D Y, Hu Z B, Wang Z S, Wang Y H, 2006. Removal of phosphate from aqueous solution by zeolite synthesized from fly ash. *Journal of Colloid and Interface Science*, 300(2): 491–497.
- Cheung K C, Venkitachalam T H, 2000. Improving phosphate removal of sand infiltration system using alkaline fly ash. *Chemosphere*, 41(1-2): 243–249.
- Farrah H, Pickering W F, 1977. The effect of pH on the retention of Cu, Pb, Zn and Cd by clay-humic acid mixtures. *Water, Air and Soil Pollution*, 14(1): 13–21.
- Guan X H, Chen G H, Shang C, 2007. Adsorption behavior of condensed phosphate on aluminum hydroxide. *Journal of Environmental Sciences*, 19(3): 312–318.
- Hartley A M, House W A, Callow M E, Leadbeater B S C, 1997. Coprecipitation of phosphate with calcite in the presence of photosynthesizing green algae. *Water Research*, 31(9): 2261–2268.
- Johansson L, Gustafsson J P, 2000. Phosphate removal using blast furnace slags and opoka-mechanisms. *Water Research*, 34(1): 259–265.
- Juan R, Hernández S, Andrés J M, Ruiz C, 2009. Ion exchange uptake of ammonium in wastewater from a sewage treatment plant by zeolitic materials from fly ash. *Journal of Hazardous Materials*, 161(2-3): 781–786.
- Mitchell J K, Bray J D, Mitchell R A, 2000. Material interactions in solid waste landfills. In: Proceedings of a Specialty Geoenvironment Conference. ASCE, New Orleans. 568–590.
- Nandi B K, Uppaluri R, Purkait M K, 2008. Preparation and characterization of low cost ceramic membranes for micro-filtration applications. *Applied Clay Science*, 42(1-2): 102–110.
- Ngah W S W, Fatinathan S, 2010. Adsorption characterization of Pb(II) and Cu(II) ions onto chitosan-tripolyphosphate beads: Kinetic, equilibrium and thermodynamic studies. *Journal of Environmental Management*, 91(4): 958–969.
- Oguz E, 2004. Removal of phosphate from aqueous solution with blast furnace slag. *Journal of Hazardous Materials*, 114(1-3): 131–137.
- Onyango M S, Kuchar D, Kubota M, Matsuda H, 2007. Adsorptive removal of phosphate ions from aqueous solution using synthetic zeolite. *Industrial & Engineering Chemistry Research*, 46(3): 894–900.
- Peterson S R, Gee G W, 1985. Interaction between acidic solutions and clay liners: permeability and neutralisation. In: Hydraulic Barriers in Soil and Rock, ASTM STP 874 (Johnson A I, Frobels R K, Cavalli N J, Pettersson C B, eds.). American Society for Testing and Materials, Philadelphia. 229–245.
- Petkowicz D I, Rigo R T, Radtke C, Pergher S B, Dos Santos J H Z, 2008. Zeolite NaA from Brazilian chrysotile and rice husk. *Microporous and Mesoporous Materials*, 116(1-3): 548–554.
- Reed E B, Vaughan R, Jiang L Q, 2000. As(III), As(V), Hg, and Pb removal by Fe-oxide impregnated activated carbon. *Journal of Environmental Engineering*, 126(9): 869–873.
- Saada M A, Soular M, Patarin J, Regis R C, 2009. Synthesis of zeolite materials from asbestos wastes: an economical approach. *Microporous and Mesoporous Materials*, 122(1-3): 275–282.
- Sakadevan K, Bavor H J, 1998. Phosphate adsorption characteristics of soils, slags and zeolite to be used as substrates in constructed wetland systems. *Water Research*, 32(2): 393–399.
- Van Reeuwijk L P, 1992. Procedures for soil analysis. International Soil Reference and Information Centre, Wageningen. 91.
- Wang S L, Cheng C Y, Tzou Y M, Liaw R B, Chang T W, Chen J H, 2007. Phosphate removal from water using lithium intercalated gibbsite. *Journal of Hazardous Materials*, 147(1-2): 205–212.
- WHO (World Health Organization), 1993. Guidelines for Drinking Water Quality. World Health Organization, Geneva.
- Wu D Y, Zhang B H, Li C J, Zhang Z J, Kong H N, 2006. Simultaneous removal of ammonium and phosphate by zeolite synthesized from fly ash as influenced by salt treatment. *Journal of Colloid and Interface*, 304(2): 300–306.
- Ye H P, Chen F Z, Sheng Y Q, Sheng G Y, Fu J M, 2006. Adsorption of phosphate from aqueous solution onto modified palygorskites. *Separation and Purification Technology*, 50(3): 283–290.
- Youssef H, Ibrahim D, Komarneni S, 2008. Microwave-assisted versus conventional synthesis of zeolite A from metakaolinite. *Microporous and Mesoporous Materials*, 115(3): 527–534.
- Zhu M X, Ding K Y, Xu S H, Jiang X, 2009. Adsorption of phosphate on hydroxyaluminum- and hydroxyiron-montmorillonite complexes. *Journal of Hazardous Materials*, 165(1-3): 645–651.

JOURNAL OF ENVIRONMENTAL SCIENCES

Editors-in-chief

Hongxiao Tang

Associate Editors-in-chief

Nigel Bell Jiuhi Qu Shu Tao Po-Keung Wong Yahui Zhuang

Editorial board

R. M. Atlas University of Louisville USA	Alan Baker The University of Melbourne Australia	Nigel Bell Imperial College London United Kingdom	Tongbin Chen Chinese Academy of Sciences China
Maohong Fan University of Wyoming Wyoming, USA	Jingyun Fang Peking University China	Lam Kin-Che The Chinese University of Hong Kong, China	Pinjing He Tongji University China
Chihpin Huang "National" Chiao Tung University Taiwan, China	Jan Japenga Alterra Green World Research The Netherlands	David Jenkins University of California Berkeley USA	Guibin Jiang Chinese Academy of Sciences China
K. W. Kim Gwangju Institute of Science and Technology, Korea	Clark C. K. Liu University of Hawaii USA	Anton Moser Technical University Graz Austria	Alex L. Murray University of York Canada
Yi Qian Tsinghua University China	Jiuhi Qu Chinese Academy of Sciences China	Sheikh Raisuddin Hamdard University India	Ian Singleton University of Newcastle upon Tyne United Kingdom
Hongxiao Tang Chinese Academy of Sciences China	Shu Tao Peking University China	Yasutake Teraoka Kyushu University Japan	Chunxia Wang Chinese Academy of Sciences China
Rusong Wang Chinese Academy of Sciences China	Xuejun Wang Peking University China	Brian A. Whitton University of Durham United Kingdom	Po-Keung Wong The Chinese University of Hong Kong, China
Min Yang Chinese Academy of Sciences China	Zhifeng Yang Beijing Normal University China	Hanqing Yu University of Science and Technology of China	Zhongtang Yu Ohio State University USA
Yongping Zeng Chinese Academy of Sciences China	Qixing Zhou Chinese Academy of Sciences China	Lizhong Zhu Zhejiang University China	Yahui Zhuang Chinese Academy of Sciences China

Editorial office

Qingcai Feng (Executive Editor) Zixuan Wang (Editor) Suqin Liu (Editor) Zhengang Mao (Editor)
Christine J Watts (English Editor)

Journal of Environmental Sciences (Established in 1989)

Vol. 24 No. 4 2012

Supervised by	Chinese Academy of Sciences	Published by	Science Press, Beijing, China
Sponsored by	Research Center for Eco-Environmental Sciences, Chinese Academy of Sciences		Elsevier Limited, The Netherlands
Edited by	Editorial Office of Journal of Environmental Sciences (JES) P. O. Box 2871, Beijing 100085, China Tel: 86-10-62920553; http://www.jesc.ac.cn E-mail: jesc@263.net , jesc@rcees.ac.cn	Distributed by	Domestic Science Press, 16 Donghuangchenggen North Street, Beijing 100717, China Local Post Offices through China Foreign Elsevier Limited http://www.elsevier.com/locate/jes
Editor-in-chief	Hongxiao Tang	Printed by	Beijing Beilin Printing House, 100083, China
CN 11-2629/X	Domestic postcode: 2-580		Domestic price per issue RMB ¥ 110.00

ISSN 1001-0742



jesc.ac.cn